Journal of Magnetic Resonance **137,** 316–323 (1999)
Article ID jmre.1998.1685, available online at http://www.idealibrary.com on IDEAL®

Time Correlations in Fluid Transport Obtained by Sequential Rephasing Gradient Pulses

Siegfried Stapf,[1] Robin A. Damion, and Ken J. Packer

Department of Chemistry, University of Nottingham, Nottingham NG7 2RD, United Kingdom

Received June 8, 1998; revised December 7, 1998

We present a basic experiment by which the evolution of the displacement probability density (propagator) of static or flowing fluid in N successive time intervals is obtained by single labeling, coupled with multiple rephasing events during the course of a pulsed field-gradient sequence. We term this type of sequence SERPENT: SEquential Rephasing by Pulsed field-gradients Encoding N Time-intervals. Realizations of the SERPENT experiment for the case $N = 2$ which include spin echo, stimulated echo, and Carr–Purcell pulse sequences are suggested. They have in common a spatial spin-labeling of the initial magnetization by a gradient of area $\mathbf{q}_0$, followed by successive rephasing via gradients $\mathbf{q}_1$ and $\mathbf{q}_2$ at times $t = \Delta_1$ and $t = \Delta_2$, respectively, where $\mathbf{q}_0 + \mathbf{q}_1 + \mathbf{q}_2 = 0$. A two-dimensional Fourier transform with respect to $\mathbf{q}_1$ and $\mathbf{q}_2$ gives directly the joint probability density $W_2(\mathbf{R}_1, \Delta_1; \mathbf{R}_2, \Delta_2)$ for displacements $\mathbf{R}_1$ and $\mathbf{R}_2$ in times Δ_1 and Δ_2, respectively. $\mathbf{q}_1$ and $\mathbf{q}_2$ may be in arbitrary directions. Assuming $\mathbf{R}_1 \| \mathbf{R}_2$, the correlation coefficient $\rho_{\mathbf{R}_1,\mathbf{R}_2}$ then reflects the time-history of the fluctuating velocities. The behavior of the cross moment $\langle \mathbf{R}_1(\Delta_1) \cdot \mathbf{R}_2(\Delta_2) \rangle$ can be obtained from either a full two-dimensional or a set of one-dimensional SERPENT measurements. Experimental results are presented for water flowing through a bed of packed glass beads. While Δ_1 is appropriately chosen to sample the short-time velocity field within the system, increasing Δ_2 clearly shows the loss of correlation when the average fluid element displacement exceeds the bead diameter.

Key Words: **time correlation; multiple rephasing; two-dimensional propagators; flow; porous media.**

INTRODUCTION

The investigation of fluid transport through porous solids by means of nuclear magnetic resonance techniques has attracted considerable interest in recent years. A method aimed at determining the statistical properties of particle displacements is based on the propagator formalism (*1*) which allows the observation of the complete probability density function in a given system (*2–5*) either parallel (Z) or perpendicular (X) to the pressure gradient. In previous work (*6, 7*), we presented a two-dimensional experiment which enabled us to determine the spatial correlation between these two displacement components. By observing the time evolution of the joint probability density $P_\Delta(X, Z)$ and quantities derived from it such as the correlation coefficient $\rho_{X^2,Z}$, it was possible to relate the properties of the fluid dispersion to characteristic sizes of the pore matrix.

In this paper we describe a family of pulsed magnetic field gradient (PFG) experiments which give direct information on the time correlation of fluid displacements. The principle of these experiments is illustrated in Fig. 1, which shows the simplest version in terms of only the gradient pulses used. The essential idea is that a gradient pulse, $\mathbf{q}_0$, applied to a spin system with transverse magnetization, phase labels spins at $t = 0$. Here, $\mathbf{q}_0 = (2\pi)^{-1}\gamma\delta_0\mathbf{g}_0$, where $\mathbf{g}_0$ and δ_0 are the strength and the duration of the gradient, respectively. Unlike the normal bipolar gradient pulse experiment, in which rephasing is accomplished by a single second gradient pulse at time $t = \Delta$ after the first, in this experiment rephasing is brought about by two gradient pulses, $\mathbf{q}_1$ at Δ_1 and $\mathbf{q}_2$ at Δ_2. The observation of a signal following the second of these pulses requires that $\mathbf{q}_0 + \mathbf{q}_1 + \mathbf{q}_2 = 0$. This division of the rephasing gradient pulse into two pulses at different times Δ_1 and Δ_2 has the effect of encoding into the final signal information on the displacement distributions in the gradient directions at both times. A generalization of this experiment is the use of N rephasing gradient pulses at times Δ_i, $i = 1 \ldots N$, for which the condition $\{\mathbf{q}_0 + \sum_{n=1}^{N} \mathbf{q}_n\} = 0$ must be observed. For evenly spaced refocusing pulses the separation of the individual pulses Δ_i can define a characteristic sampling frequency Δ_i^{-1} which may be chosen as the variable in a diffusion or flow experiment, as was suggested in (*8*).

We propose as an acronym for these experiments: SERPENT (SEquential Rephasing by Pulsed field-gradients Encoding N Time intervals).

THEORY

We will assume the principal scheme of the experiment outlined above (see Fig. 1). Subject to the condition $\mathbf{q}_0 + \mathbf{q}_1 + \mathbf{q}_2 = 0$, the gradients can be chosen to have arbitrary values; in particular, $|\mathbf{q}_1|, |\mathbf{q}_2| > |\mathbf{q}_0|$ is allowed. Arising from the first gradient pulse, each nuclear spin i experiences a phase shift ϕ_i

[1] To whom correspondence should be addressed. Fax: +44-115-951-3562; E-mail: pczssx@unix.ccc.nottingham.ac.uk.

1090-7807/99 $30.00

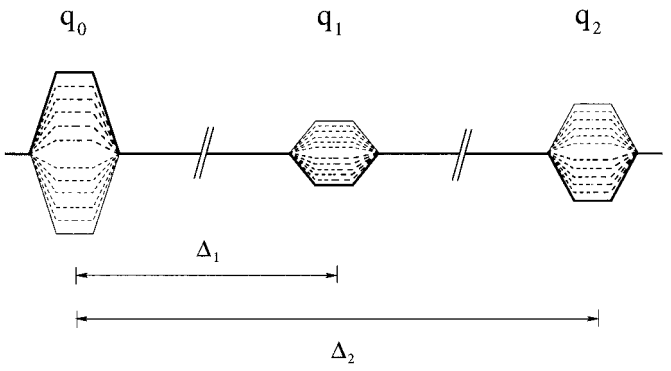

FIG. 1. Basic scheme of the SERPENT experiment. The effective gradients must meet the condition $\mathbf{q}_0 + \mathbf{q}_1 + \mathbf{q}_2 = 0$.

that is proportional to its position at time 0 and to the area of the gradient,

$$\phi_i[\mathbf{g}_0, \delta_0, \mathbf{r}_i(0)] = \delta_0\omega[\mathbf{r}_i(0)] = \delta_0\{\gamma B_0 + \gamma\mathbf{g}_0 \cdot \mathbf{r}_i(0)\}, \quad [1]$$

where B_0 denotes the static magnetic field. After the evolution time Δ_2, provided that $\delta_i \ll \Delta_i$, the rephasing gradients have the effect of an additional phase shift which leaves the resultant shift

$$\phi_i(\Delta_2) = \gamma\{\delta_0\mathbf{g}_0 \cdot \mathbf{r}_i(0) + \delta_1\mathbf{g}_1 \cdot \mathbf{r}_i'(\Delta_1) + \delta_2\mathbf{g}_2 \cdot \mathbf{r}_i''(\Delta_2)\}. \quad [2]$$

The total signal amplitude is obtained by summation over all spins, equivalent to the following integral, where the replacement $\mathbf{q}_i = (2\pi)^{-1}\gamma\delta_i\mathbf{g}_i$ has been made:

$$S(\mathbf{q}_1, \mathbf{q}_2) = \int\int\int P_3(\mathbf{r}, 0; \mathbf{r}', \Delta_1; \mathbf{r}'', \Delta_2) \times e^{i2\pi[\mathbf{q}_0\cdot\mathbf{r} + \mathbf{q}_1\cdot\mathbf{r}' + \mathbf{q}_2\cdot\mathbf{r}'']} d\mathbf{r}\, d\mathbf{r}'\, d\mathbf{r}''. \quad [3]$$

$P_3(\mathbf{r}, 0; \mathbf{r}', \Delta_1; \mathbf{r}'', \Delta_2)$ is the joint probability density of finding particles at $\mathbf{r}$, $\mathbf{r}'$, and $\mathbf{r}''$ at the given times. As an experiment necessarily averages over all starting positions (*9*), we define an averaged two-time probability density as follows, making use of the replacement $\mathbf{q}_0 = -\mathbf{q}_1 - \mathbf{q}_2$,

$$S(\mathbf{q}_1, \mathbf{q}_2) = \int\int W_2(\mathbf{R}_1, \Delta_1; \mathbf{R}_2, \Delta_2) \times e^{i2\pi\mathbf{q}_1\cdot\mathbf{R}_1} e^{i2\pi\mathbf{q}_2\cdot\mathbf{R}_2} d\mathbf{R}_1 d\mathbf{R}_2, \quad [4]$$

where $\mathbf{R}_1 = \mathbf{r}' - \mathbf{r}$ and $\mathbf{R}_2 = \mathbf{r}'' - \mathbf{r}$. $W_2(\mathbf{R}_1, \Delta_1; \mathbf{R}_2, \Delta_2)$ now represents a joint probability density for displacements $\mathbf{R}_1$ and $\mathbf{R}_2$ in times Δ_1 and Δ_2, respectively. It can be obtained directly by Fourier transformation of $S(\mathbf{q}_1, \mathbf{q}_2)$ with respect to $\mathbf{q}_1$ and $\mathbf{q}_2$. This function can only be separated into a product of two one-time probability density functions P_{Δ_i} if no correlation between displacements at Δ_1 and Δ_2 exists, i.e., if the displacement of a particle $\mathbf{R}_2$ at $t = \Delta_2$ does not depend on its displacement $\mathbf{R}_1$ at $t = \Delta_1$. A generalization toward an N-time probability density function W_N is straightforward.

Note that the orientations of $\mathbf{q}_1$ and $\mathbf{q}_2$ are arbitrary. Although one might usually be interested in displacements along the same direction, it is also possible to compare the displacements in one direction with those along a perpendicular axis at an earlier time.

It should be pointed out that the method presented here aims at monitoring the continuous evolution of displacement probability densities, while the VEXSY (velocity exchange spectroscopy) experiment discussed in (*10*) correlates displacements during two intervals separated from each other. However, the VEXSY method can be regarded as a special case of the SERPENT experiment with $N = 3$ and with the additional conditions $\mathbf{q}_0 + \mathbf{q}_1 = 0$ and $\mathbf{q}_2 + \mathbf{q}_3 = 0$, where full rephasing is achieved following $\mathbf{q}_1$ as well as $\mathbf{q}_3$. In (*11*), a similar method is suggested, which, employing the same conditions, derives information about local pore anisotropies from two separated encoding/decoding steps with a varying angle between the gradient directions of both steps.

If one were satisfied with obtaining only the time evolution of the second moment of the displacement correlation, $\langle\mathbf{R}_1(\Delta_1) \cdot \mathbf{R}_2(\Delta_2)\rangle$, the full experiment described above can be replaced by a set of one-dimensional measurements employing the identical method. Using the composite variable $\boldsymbol{\xi} = f_1\mathbf{R}_1(\Delta_1) + f_2\mathbf{R}_2(\Delta_2)$, where $\mathbf{q}_i = -f_i\mathbf{q}_0$, $f_1 + f_2 = 1$ and all gradients are parallel to each other, Eq. [4] can be rewritten as

$$S(f_1, f_2) = \int P(\boldsymbol{\xi}) e^{i2\pi\mathbf{q}_0\cdot\boldsymbol{\xi}} d\boldsymbol{\xi}. \quad [5]$$

The second moment of $P(\boldsymbol{\xi})$ has the form $\langle\boldsymbol{\xi}^2\rangle = \langle f_1^2\mathbf{R}_1^2 + f_2\mathbf{R}_2^2 + 2f_1f_2\mathbf{R}_1 \cdot \mathbf{R}_2\rangle$. Measuring $\langle\boldsymbol{\xi}^2\rangle$ for, say, $f_1 = f_2 = \frac{1}{2}$, by variation of and Fourier transformation with respect to $\mathbf{q}_0$, allows the determination of $\langle\mathbf{R}_1 \cdot \mathbf{R}_2\rangle$ once $\langle\mathbf{R}_1^2\rangle$ and $\langle\mathbf{R}_2^2\rangle$ are known either by separately setting f_1 to 0 and 1 or from conventional PFG experiments. Like the full two-time probability density function, this method can easily be extended to the general case of N rephasing gradient pulses, which will give access to higher order displacement correlation functions.

EXPERIMENTAL

The simplest possible realization of the SERPENT experiment is shown in Fig. 2a and consists of a Pulsed Gradient Spin Echo (PGSE) sequence with appropriately placed field gradients. The longest accessible timescale, Δ_2, is determined by the homogeneity of the magnetic field and the transverse relaxation

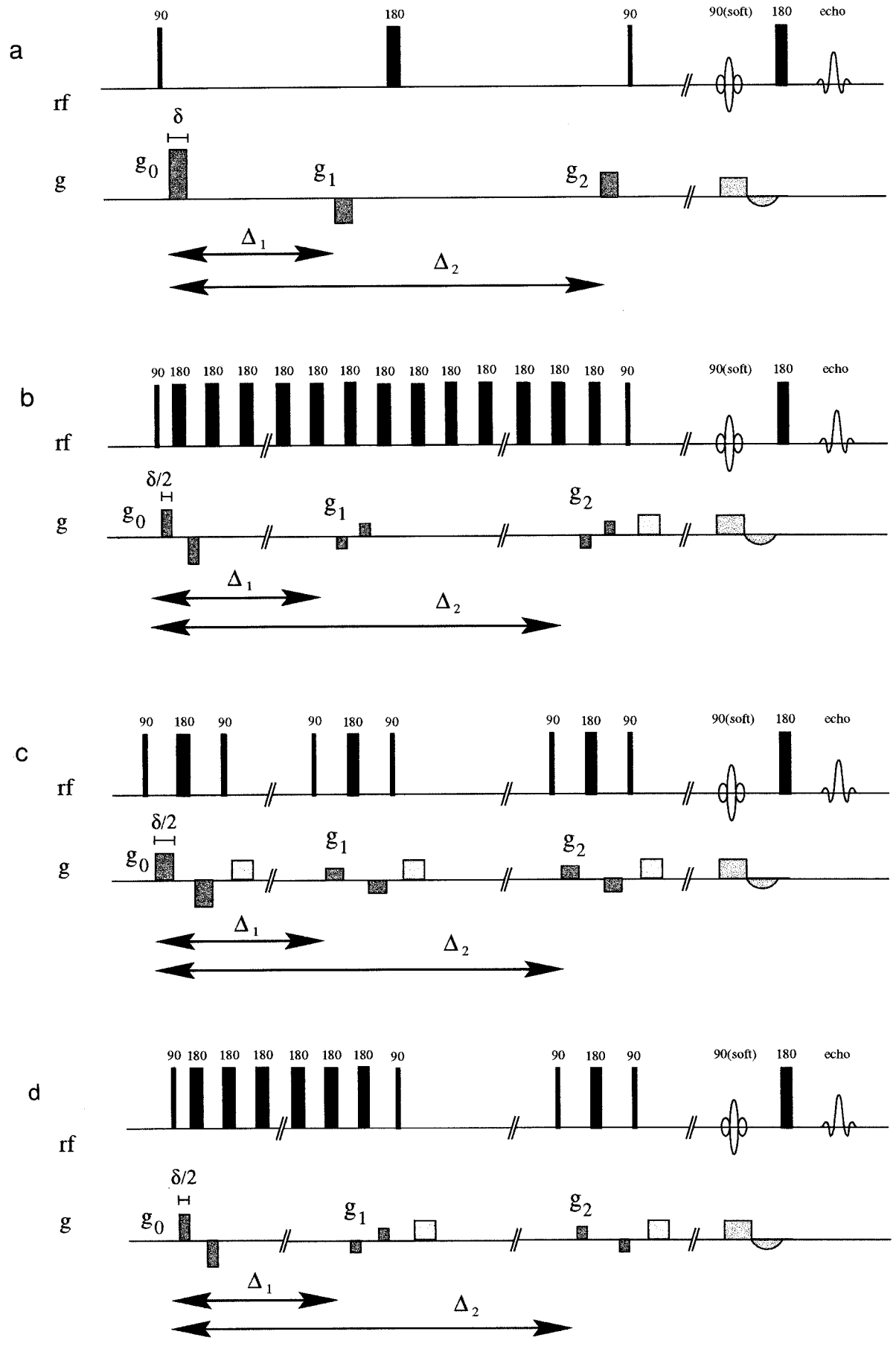
a
90
180
90
90(soft)
180
echo
rf
δ
g
g0
g1
g2
Δ1
Δ2
b
90 180 180 180 180 180 180 180 180 180 180 180 180 180 90
90(soft)
180
echo
rf
δ/2
g
g0
g1
g2
Δ1
Δ2
c
90 180 90 90 180 90 90 180 90
90(soft)
180
echo
rf
δ/2
g
g0
g1
g2
Δ1
Δ2
d
90 180 180 180 180 180 180 90 90 180 90
90(soft)
180
echo
rf
δ/2
g
g0
g1
g2
Δ1
Δ2

time T_2. The presence of a background gradient **G** will lead not only to an additional signal decay but also to cross-terms of the form $\mathbf{G} \cdot \mathbf{g}_i$ which affect the phase and the intensity of the signal acquired at $t = \Delta_2$ in a different way for any combination of $\mathbf{g}_1$ and $\mathbf{g}_2$.

The influence of background gradients can be suppressed by applying a Carr–Purcell sequence and inserting pulsed gradients at the desired time intervals (see Fig. 2b). Best results are achieved by splitting each pulse $\mathbf{g}_i$ into two (or more) components of opposite sign separated by an RF π pulse. By this method, all components add up to an effective gradient while the constant background contribution is eliminated and cross-terms are significantly reduced (*12*). A suitable compensated CPMG sequence such as the XY-8 variety (*13*) must be used in order to preserve both orthogonal components of the magnetization.

In cases where $T_1 \gg T_2$ is found, e.g., for fluids in porous media, long timescales can best be probed by observing the stimulated echo. Figure 2c shows a modification of the APGSTE sequence (*2, 14*). A second gradient pulse pair sandwiched between an RF pulse triplet is added to allow the application of all three gradients $\mathbf{g}_i$ while the magnetization is stored in the longitudinal direction between these periods. The spin system is only subject to T_2 relaxation between each $\pi/2$ RF pulse pair.

In practice, the SERPENT experiment will often be performed employing a suitably chosen short interval Δ_1 and a series of Δ_2 values. Therefore, T_2 relaxation might not be relevant within Δ_1. As a hybrid method, we have used the sequence shown in Fig. 2d, in which the magnetization is evolving in the transverse plane until after the second gradient pulse pair, while the delay between $\mathbf{g}_0$ and $\mathbf{g}_1$ is bridged by a Carr–Purcell train of RF pulses. As in all previous applications to porous media, the condition $\langle \mathbf{R}_i^2(\delta) \rangle \ll a^2$, where a is the pore size, must be met.

The measurements presented here were carried out using a GEΩ CSI spectrometer operating for proton resonance at 85 MHz, the field being provided by an Oxford Instruments 85/310 horizontal bore magnet equipped with room temperature shims and S-150 Acustar actively shielded gradient coils providing gradients of up to 2.0 T m^{-1}. Phase cycling of the RF pulses (*14*) was used to minimize the effects of background gradients and dc offsets.

A glass tube of 11 mm i.d. and 200 mm length was filled with a suspension of water and glass beads of $d = 300$ μm average diameter; the bead packing was slightly compacted but not centrifuged. Copper(II)-sulfate was added to the flowing water in order to allow a repetition time of 1.0 s. The water flow was driven by a precision pump (Pharmacia P50) which was operated at constant volume flow rates of 7.0 and 14.0 ml/min, respectively. These flow rates correspond to Reynolds and Peclet numbers which allow comparison with previously obtained experimental data and numerical simulations (*7*). Experiments presented here were performed using the pulse sequence given in Fig. 2d. The signal was acquired on a slice of 10 mm thickness at the center of the sample. Two-dimensional data sets were obtained by stepwise variation of the strength of the pulsed field-gradients $\mathbf{q}_1$ and $\mathbf{q}_2$ while the value of $\mathbf{q}_0$ was calculated from them. An experiment consisted typically of 32×32 symmetrical steps covering the range $\pm\mathbf{q}_{1,max}$ and $\pm\mathbf{q}_{2,max}$. The two-dimensional data set was then Fourier-transformed numerically and subsequently phase-corrected. The marginals $P_{\Delta_1}(Z_1)$ and $P_{\Delta_2}(Z_2)$ of the resulting propagator $W_2(Z_1, \Delta_1; Z_2, \Delta_2)$, defined as

$$P_{\Delta_1}(Z_1) = \int W_2(Z_1, \Delta_1; Z_2, \Delta_2) dZ_2,$$

$$P_{\Delta_2}(Z_2) = \int W_2(Z_1, \Delta_1; Z_2, \Delta_2) dZ_1, \qquad [6]$$

were compared to one-dimensional propagators obtained under identical conditions but with a higher resolution of 64 or 128 points. The propagators matched satisfactorily.

RESULTS AND DISCUSSION

In our previous work, we investigated the spatial two-dimensional propagator $P_\Delta(X, Z)$ for a similar system of packed glass beads (*7*). We found that the correlation coefficient for displacements parallel and perpendicular to the pressure gradient, $\rho_{X^2,Z}$, reached a maximum value at average displacements corresponding to one bead radius. Larger displacements led to a decrease of $\rho_{X^2,Z}$ because of the dispersion process and the mixing of particles between different streamlines, while for much smaller displacements, diffusion was dominating. This can also be seen in the one-dimensional propagator $P_\Delta(Z)$ (*2, 15*): for short encoding times Δ, the propagator is essentially Gaussian in shape and the particle displacements are dominated by their Brownian motion, given by the self-diffusion coefficient D_0. Only for longer times does the shape of the spreading function deviate significantly from the case of self-diffusion.

As we want to investigate how displacements after an interval Δ_1 have evolved at a later time Δ_2, we are interested in

FIG. 2. Four different realizations of the basic SERPENT experiment as described in the text. (a) Pulsed Gradient Spin Echo (PGSE) sequence with two rephasing gradient pulses. (b) Carr–Purcell–Meiboom–Gill (CPMG) sequence with split gradient pairs. For gradient signs as in this figure, an even number of π pulses between the gradient elements is required. (c) Alternate Pulsed Gradient STimulated Echo (APGSTE) sequence with two rephasing steps. (d) APGSTE sequence with CPMG module during the first evolution interval.

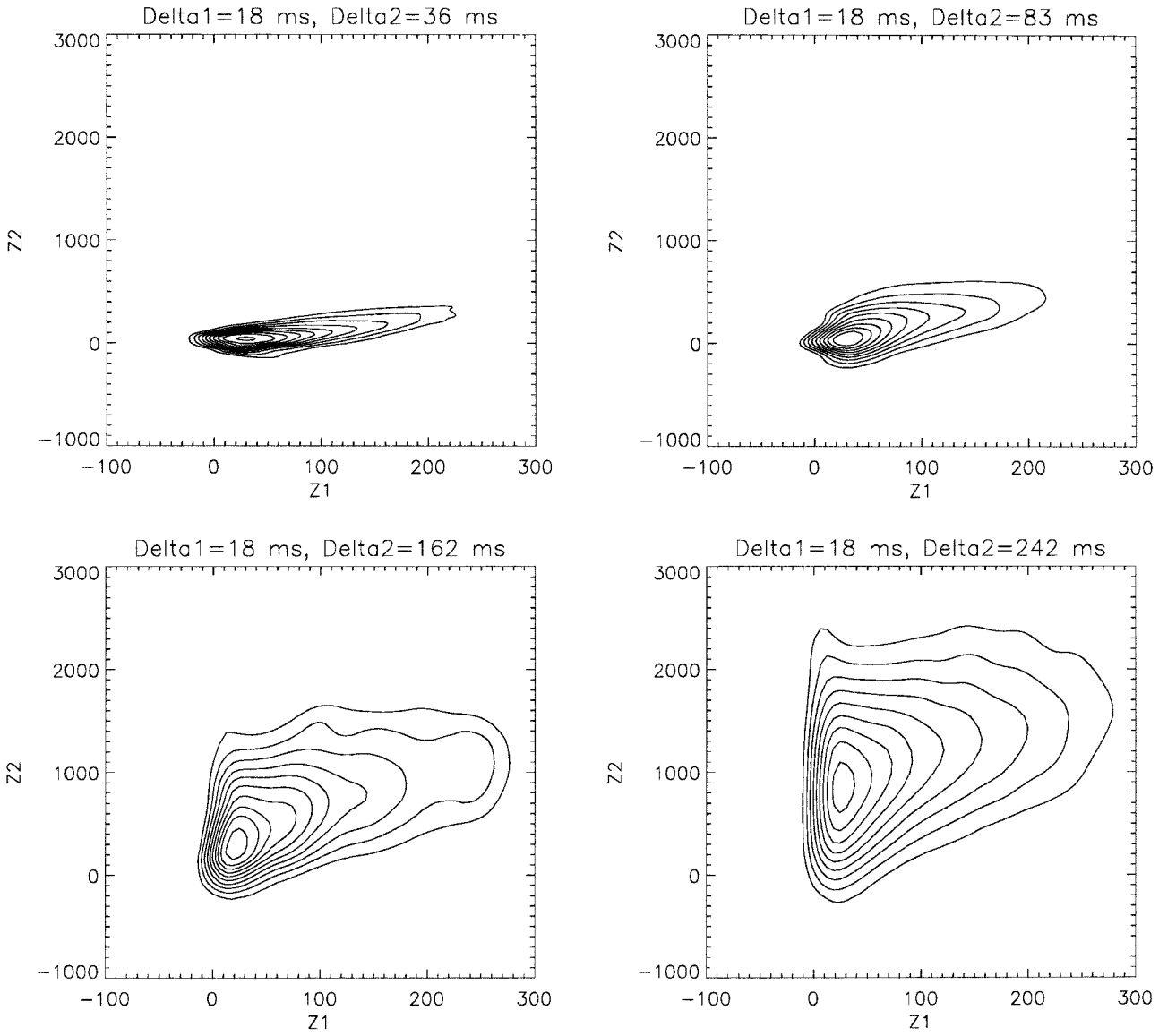

FIG. 3. Two-time probability density function $W_2(Z_1, \Delta_1; Z_2, \Delta_2)$ for water flowing with $Q = 14.0$ ml/min in a bed of glass beads of 300 μm diameter. $\Delta_1 = 18$ ms is held constant; Δ_2 is varied as indicated. Axis labels correspond to displacements in μm.

defining a suitable value for Δ_1 which best represents the velocity field within the porous matrix. From the findings in (*7*), this means combining the two conditions $\langle Z_1^2(\Delta_1)\rangle \gg 2D_0\Delta_1$ and $\langle Z_1(\Delta_1)\rangle < d/2$, where d is the bead diameter, with the restrictions given by experimental time and available flow rate. We have chosen $\Delta_1 = 30$ ms for a flow rate of 7.0 ml/min and $\Delta_1 = 18$ ms for 14.0 ml/min, corresponding to average displacements $\langle Z_1(\Delta_1)\rangle$ of 70 and 85 μm, respectively.

It should be pointed out that for the complete evaluation of the two-time propagator $W_2(Z_1, \Delta_1; Z_2, \Delta_2)$, both Δ_1 and Δ_2 must be varied over an appropriate range of times, resulting in a four-dimensional space of two displacement dimensions and two time dimensions each. For practical reasons, we have only sampled a finite number of 2-d propagator arrays (in this case about 8 values of Δ_2) within the 3-d subspace characterized by one particular Δ_1.

In Fig. 3, four examples of the function $W_2(Z_1,\Delta_1; Z_2, \Delta_2)$ are shown for $Q = 14.0$ ml/min and $\Delta_1 = 18$ ms. Displacements Z_1 parallel to the pressure gradient during the first interval Δ_1 are shown along the abscissa, while $Z_2(\Delta_2)$ are drawn along the ordinate axis. At short Δ_2, a correlation can clearly be seen: large displacements during Δ_2 are found for large displacements during Δ_1. Assuming that $P_{\Delta_1}(Z_1)$ represents the velocity field in the sample before mixing has become effective, it can be concluded that a given displacement is proportional to the particle velocity, which has not changed considerably during Δ_1. For $\Delta_2 = 36$ ms, this is still essentially

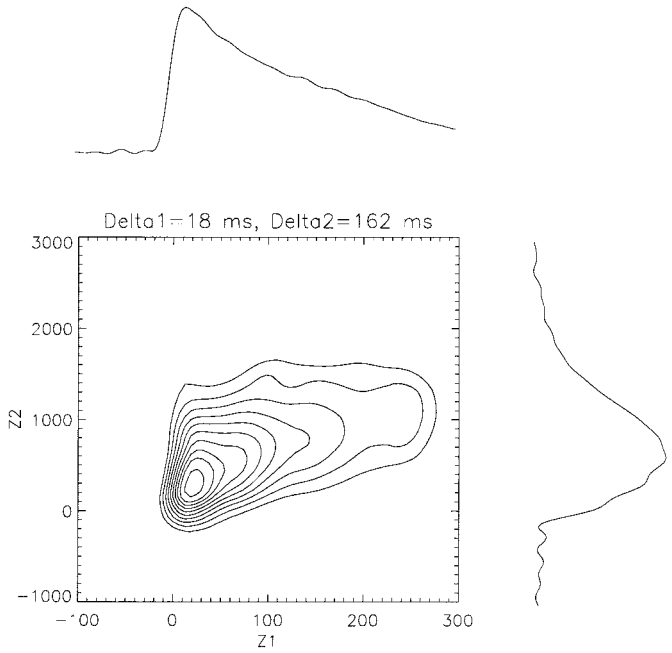

FIG. 4. Two-time probability density function $W_2(Z_1, \Delta_1; Z_2, \Delta_2)$ and marginals $P_{\Delta 1}(Z_1)$ and $P_{\Delta 2}(Z_2)$, respectively, for $\Delta_2 = 162$ ms. Experimental data are as in Fig. 3. Axis labels correspond to displacements in μm.

true. As Δ_2 is increased, the correlation becomes lost more and more; at $\Delta_2 = 242$ ms, the probability of finding a certain displacement Z_2 becomes almost independent of Z_1. This fact can be interpreted by a change in velocity for most particles; e.g., particles having a large velocity after Δ_1 have, for large Δ_2, changed streamlines to the extent that, at Δ_2, they possess almost any velocity existing within the system, weighted only by the overall distribution of velocities. This process is completed as $\Delta_2 \to \infty$.

A qualitative picture can be obtained by looking at the marginals of the probability density function $W_2(Z_1, \Delta_1; Z_2, \Delta_2)$. These are shown for one example in Fig. 4. The marginals, representing the one-dimensional propagator $P_{\Delta_i}(Z_i)$, can also be obtained by a simple APGSTE experiment (*2*, *15*). However, higher dimension propagators contain more complete information on particle displacement correlations.

The ability to correlate displacements in different directions at different times is exemplified by the correlation between $Z_1(\Delta_1)$ and $X_2(\Delta_2)$ for two evolution times, shown in Fig. 5. With growing Δ_2, the fluid particles spread in the direction perpendicular to the pressure gradient. The evolution of $W_2(Z_1, \Delta_1; X_2, \Delta_2)$, however, is less obvious at first sight. An analysis in terms of conditional probability densities shows that—as was already found in (*7*)—large values of $Z_1(\Delta_1)$ are correlated with large values of $|X_2(\Delta_2)|$. Again, this correlation decays for increasing Δ_2.

The evolution of correlations can be described in a quantitative way by employing the mathematical definition of the correlation coefficient which relates two parameters A and B, $\rho_{A,B}$,

$$\rho_{A,B} = \frac{\mathrm{cov}(A, B)}{\sqrt{\mathrm{Var}(A)}\ \sqrt{\mathrm{Var}(B)}}, \qquad [7]$$

where the covariance is defined as $\mathrm{cov}(A, B) = \langle AB \rangle - \langle A \rangle \langle B \rangle$, and $\mathrm{Var}(A)$ is the variance of A.

The first example (Fig. 3) involved the correlation between $Z_1(\Delta_1)$ and $Z_2(\Delta_2)$, and Fig. 6 shows the coefficient ρ_{Z_1,Z_2} for both flow rates as a function of the average displacement during Δ_2, $\langle Z_2 \rangle$, which in turn is proportional to the elapsed time Δ_2. As the experiments were performed with a limited resolution, the propagators are subject to considerable system-

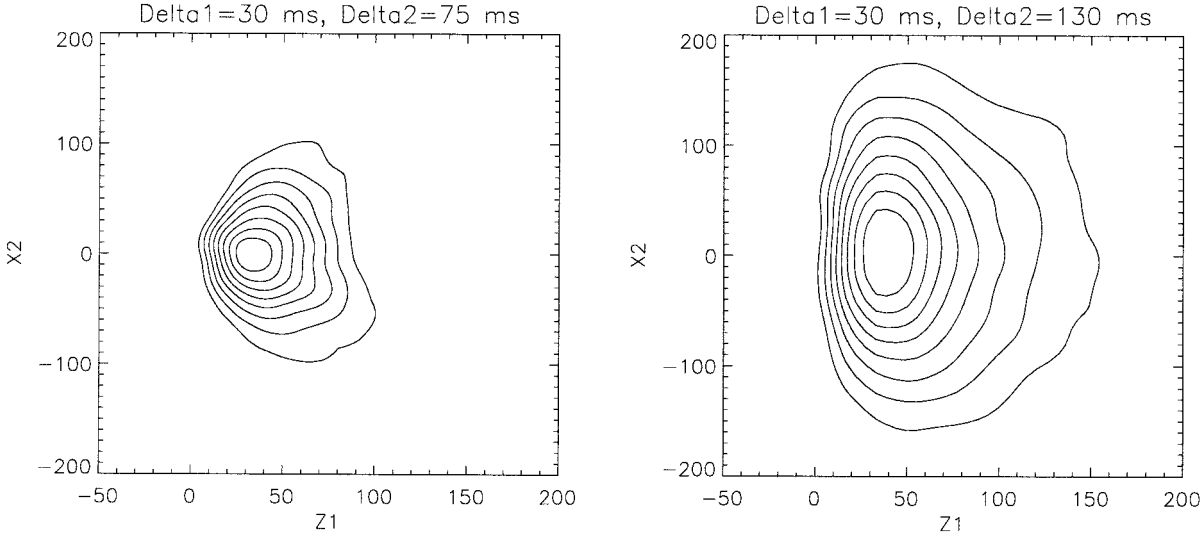

FIG. 5. Two-time probability density function $W_2(Z_1, \Delta_1; X_2, \Delta_2)$ for a flow rate of $Q = 7.0$ ml/min. Displacements in the z-direction after Δ_1 are drawn along the abscissa, displacements in the x-direction after Δ_2 along the ordinate axis. Axis labels correspond to displacements in μm.

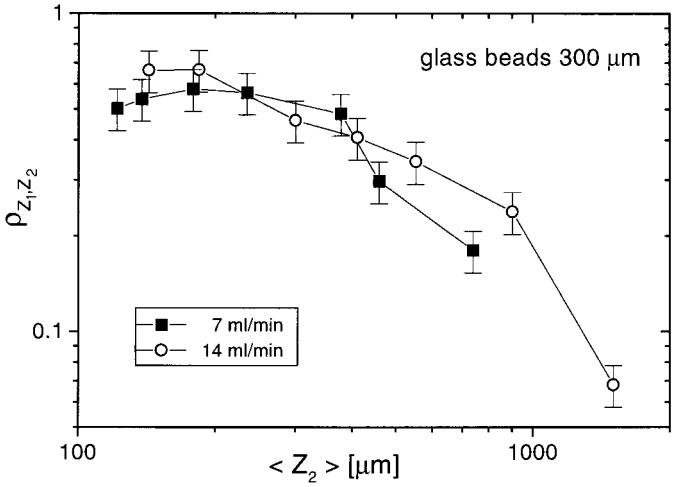

FIG. 6. Correlation coefficient ρ_{Z_1,Z_2} for water flowing in a bed of glass beads of 300 μm diameter. Error bars are estimated from repeated measurements under identical conditions.

atic fluctuations; by comparing the reproducibility of identical measurements we estimate an average error on ρ of $\pm 15\%$. Within this error margin, ρ_{Z_1,Z_2} remains roughly constant for small average displacements and decreases strongly for $\langle Z_2 \rangle > d$. The initial value between 0.5 and 0.7 is mainly a consequence of the contribution of Brownian motion to the propagator. As would be expected, the larger flow rate results in a higher initial correlation coefficient. In the absence of self-diffusion, which is equivalent to an infinite Peclet number, the correlation coefficient can be expected to reach unity for short evolution times:

$$\lim_{\mathrm{Pe}\to\infty} \lim_{\Delta_i \to 0} \rho_{Z_1,Z_2} = 1. \qquad [8]$$

In a real system where $D_0 > 0$, the highest possible value of ρ_{Z_1,Z_2} is found for a suitable choice of Δ_1 and for short Δ_2. The evolution of ρ_{Z_1,Z_2} indicates the correlation length characteristic for the system and the form of the decay contains information on the detailed characteristics of the loss in coherence of the particles' average flow paths.

CONCLUSIONS

We have presented the SERPENT experiment, a method which allows the correlation of the full displacement spectrum for a fluid at a given short encoding time with the spectrum at N later times via independent variation of the strength of N rephasing gradients, $\mathbf{q}_i$. The initial dephasing gradient $\mathbf{q}_0$ defines the beginning of the time-evolution. The N-time probability density of displacements (propagator) $W_N(\mathbf{R}_1, \Delta_1; \ldots; \mathbf{R}_N, \Delta_N)$ is obtained by Fourier transformation with respect to all $\mathbf{q}_i$, $i > 0$. The simplest and most important application of the SERPENT experiment is found for rephasing in two steps, $N = 2$. As an example, we have investigated water flowing through a packed bed of monosized spherical particles. By adjusting the first encoding time interval, Δ_1, so that the propagator $P_{\Delta_1}(\mathbf{R}_1)$ closely represents the velocity field of the system, we have measured $W_2(Z_1, \Delta_1; Z_2, \Delta_2)$ over a range of Δ_2. The loss of correlation in the particle displacement distributions between Δ_1 and Δ_2 is documented by the decay of the correlation coefficient between the displacements after both times, ρ_{Z_1,Z_2}. A map of $W_2(Z_1, \Delta_1; X_2, \Delta_2)$, correlating orthogonal displacements at different times, was shown for comparison.

The class of experiments presented here enables one to directly map the intermediate-time behavior of fluid dispersion in arbitrary environments. The decay of coherence in flow is directly related to the sampling of the porous matrix by the fluids; following the time evolution of this decay therefore allows one to define characteristic time and length scales which describe the fluid/solid interaction process. A further application will be the monitoring of the mixing process between two flowing liquids.

Performing experiments as described in this work for flow through macroscopically anisotropic samples allows the determination of order parameters of the matrix structure. The results for water flow through glass bead packings are in good agreement with earlier investigations of correlations at single times, but orthogonal directions (*7*). In this work, correlations between displacements parallel and perpendicular to the flow axis were found to be high for short encoding times but to decay when the average displacement exceeded the pore size.

Further detailed experiments and numerical simulations have been performed for several porous systems and will be published elsewhere (*16*). The investigations of time-correlated displacement spectra represent a potentially powerful tool for the understanding of complex flow processes in the presence of sorption, exchange, and chemical reactions. A combination of both methods seems suitable for a further understanding of the properties of the spreading of fluids in inhomogeneous media in general and flow and dispersion in porous solids in particular.

ACKNOWLEDGMENTS

Financial support from the EPSRC is gratefully acknowledged. One of us (S.S.) is indebted to the Deutsche Forschungsgemeinschaft (DFG), Grant Sta 511/1-1, and the Training and Mobility of Researchers (TMR) program of the European Union, Marie Curie Fellowship Grant ERBFMBICT961836. We thank R. G. Graham and J. H. Naish for their helpful contributions in the course of the preparation and discussion of the experiments.

REFERENCES

1. J. Kärger and W. Heink, *J. Magn. Reson.* **51,** 1 (1983).
2. K. J. Packer and J. J. Tessier, *Mol. Phys.* **87,** 267 (1996).
3. M. H. G. Amin, S. J. Gibbs, R. J. Chorley, K. S. Richards, T. A. Carpenter, and L. D. Hall, *Proc. R. Soc. London A* **453,** 489 (1997).
4. J. D. Seymour and P. T. Callaghan, *AIChE J.* **43,** 2096 (1997).

5. J. J. Tessier and K. J. Packer, *Phys. Fluids* **10,** 75 (1998).

6. K. J. Packer, S. Stapf, J. J. Tessier, and R. A. Damion, *Magn. Reson. Imaging* **16,** 463 (1998).

7. S. Stapf, K. J. Packer, R. G. Graham, J.-F. Thovert, and P. M. Adler, *Phys. Rev. E* **58,** 6206 (1998).

8. P. T. Callaghan and J. Stepišnik, *Adv. Opt. Magn. Reson.* **19,** 325 (1996).

9. P. T. Callaghan, "Principles of Nuclear Magnetic Resonance Microscopy," Clarendon Press, Oxford (1991).

10. P. T. Callaghan and B. Manz, *J. Magn. Reson. A* **106,** 260 (1994).

11. P. P. Mitra, *Phys. Rev. B* **51,** 15074 (1995).

12. R. M. Cotts, M. J. R. Hoch, T. Sun, and J. T. Marker, *J. Magn. Reson.* **83,** 252 (1989).

13. T. Gullion, D. B. Baker, and M. S. Conradi, *J. Magn. Reson.* **89,** 479 (1990).

14. E. J. Fordham, S. G. Gibbs, and L. D. Hall, *Magn. Reson. Imaging* **12,** 279 (1994).

15. J. J. Tessier, K. J. Packer, J.-F. Thovert, and P. M. Adler, *AIChE J.* **43,** 1653 (1997).

16. S. Stapf and K. J. Packer, *Appl. Magn. Reson.,* in press.